Electronic Supplementary Material (ESI) for Physical Chemistry Chemical Physics.

Supplementary information

Understanding chemical interaction between phosphonate-derivative molecules and silver surface cluster in SERS: a combined experimental and computational approach

Gauthier Emonds-Alt,[ab] Benoit Mignolet,[c] Cédric Malherbe,[a] Jean-Christophe M. Monbaliu,[b]
Françoise Remacle,[c] and Gauthier Eppe[a]

a) Mass Spectrometry Laboratory, MolSys Research Unit, University of Liège, B4000 Liège, Belgium
b) Center for Integrated Technology and Organic Synthesis, MolSys Research Unit, University of Liège, B4000 Liège, Belgium.
c) Theoretical Physical Chemistry, MolSys Research Unit, University of Liège, 4000 Liege, Belgium.

Summary

1) Explicit solvation

2) Isomers of the analyte-silver cluster complexes

3) Raman spectra between 0 and 2000 cm^{-1}

1) Explicit solvation

The explicit interaction of water molecules with the analytes investigated in this paper is important in SERS, particularly for the methyl phosphonate and the AMPA molecules. Using a PCM model that accounts for the polarization of the analyte due to the solvent but not for the hydrogen bonding, we observed discrepancies between the computed and measured spectra. Namely, the computed vibrational frequency of the P-C stretching is lower compared to the experimental one (red shifted by ≈ 50 cm^{-1}) and the relative intensity of the symmetric and antisymmetric P-O stretching bands is not well described (Fig. 2B and D). We investigate the effect of explicitly adding water molecules for the $MePO_3^{2-}$ analyte because it has a single binding site and no acidic proton. It is therefore likely that the discrepancies between the computed and measured spectra arise from using a continuous medium description of the solvation. We therefore report below computed Raman spectrum obtained with explicit solvation with H_2O molecules. We first report on explicit solvation of the isolated methyl phosphonate anion because it is possible to add a complete solvation shell around the analyte while it is currently computationally out of range for the nanometer sized complex $(Ag_{20}\text{-}MePO_3)^{2-}$. Then we report the Raman spectrum of the $(Ag_{20}\text{-}MePO_3)^2$ complex solvated with 3 water molecules.

As the experimental SERS spectrum (Figure 2 and S2A), the experimental Raman spectrum of the isolated analyte has 3 main bands between 600 and 1450 cm^{-1} (Fig. S1A). The computed peak of the methyl breathing (1400 cm^{-1}) of the isolated $MePO_3^{2-}$ anion (Figure S1 D) is well described but the P-C stretching peak is red shifted by 100 cm^{-1} compared to the experimental spectrum (750 cm^{-1} in the experimental spectrum). In addition, the computed P-O stretching band (between 800 and 1100 cm^{-1}) is composed of three peaks while only one is observed experimentally (with a small side peak). To assess the effect of explicit solvation on the Raman spectrum, we added water molecules close to the $MePO_3^{2-}$ anion in addition to the implicit solvation model. We first added 3 water molecules close to the oxygen atoms of the phosphonate (Figure S1C) and then added a full solvation shell of 25 water molecules (Fig. S1B). When adding 3 H_2O molecules close to the phosphonate, we observe the formation of hydrogen bonds with the oxygen atoms of the phosphonate, which leads to a decrease of the NBO charge of the oxygen atoms from -1.27 to -1.22. In addition, the P-C bond has a more ionic character, which translates by a shortening of the bond (from 1.89 Å to 1.84 Å) and a blue shift of the computed P-C bond stretching frequency from 650 cm^{-1} to 710 cm^{-1}. Adding explicit solvation to an implicit solvation model such as PCM has been shown to lead to a blue shift of the vibrational frequencies.[1] However the P-C Raman band is still red shifted compared to experimental spectrum. For the three P-O bands localized between 800 and 1100 cm^{-1}, there is a shifting of the third band from 1100 to 1050 cm^{-1} because the antisymmetric P-O stretching normal mode is now composed of a small component of bending of the water molecules. Nevertheless, there is no significant improvement of the P-O bands.

In order to obtain a qualitative agreement between the experimental and computed Raman spectrum of the $MePO_3^{2-}$ anion in solution, we need to add a solvation shell that surrounds completely the molecule (with 25 water molecules, see Figure S1 B). The addition of 25 water molecules leads to a decrease of the partial charge on the oxygen atoms and a shortening of the computed P-C bond that is now 0.08 Å shorter (1.81 Å) than for the anion computed without explicit solvation. This induces an additional blue shift of the P-C band (from 710 to 750 cm^{-1}) that is now in very good agreement with the experimental spectrum. Overall all the bands of the computed Raman spectrum are in good agreement with the experimental spectrum. Therefore, we conclude that the redshift of the P-C band and the poor description of the P-O bands are due to the sole use of the PCM model that cannot describe the hydrogen bonding between the water molecules and the analyte.

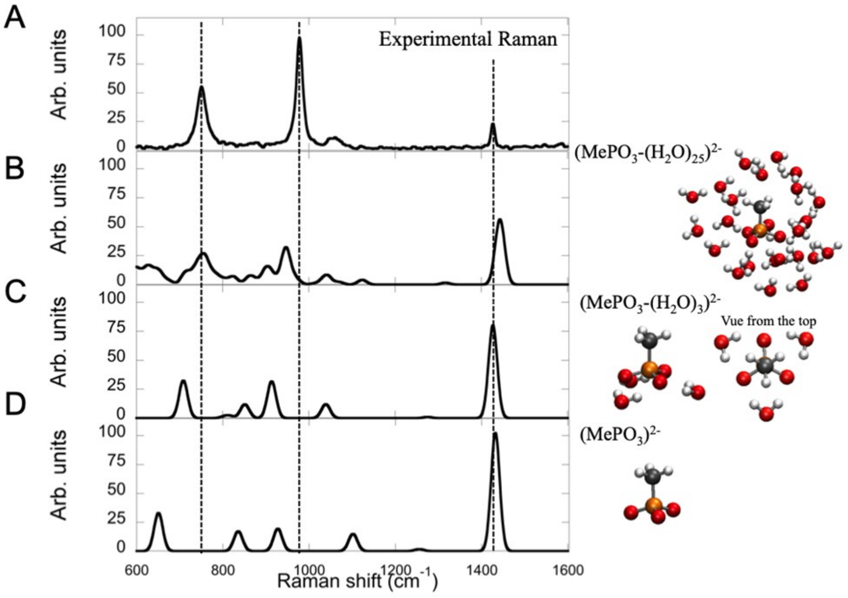

Fig S1: A) Experimental Raman spectrum of the methylphosphonate anion in solution (without NPs) at pH=9 where there is mainly the $MePO_3^{2-}$ form in solution. B-D) Raman spectrum of the $(MePO_3(H_2O)_{25})^{2-}$ complex (B), $MePO_3(H_2O)_3)^{2-}$ complex (C) and $MePO_3^{2-}$ anion (D) computed at the DFT/wB97XD level with the PCM model. The equilibrium geometries are shown on the right of the Raman spectra. The relative intensities are normalized to the highest peak for the experimental spectrum (P-O peak, panel A). For the computed spectra, the relative intensities are normalized to the peak of the methyl breathing mode (panel D).

To investigate the effect of hydrogen bonding on the computed Raman spectra of the $(Ag_{20}\text{-}MePO_3)^{2-}$ complex, we explicitly added 3 water molecules close to the oxygen atoms of the phosphonate function (Figure S2B). As in the Raman spectra of the isolated analyte, we observe a blue shift of the P-C band, which is now in good agreement with the experiment band, and no significant changes in relative intensity of the P-O bands. A better description of the P-O bands would be obtained by solvating completely the $(Ag_{20}\text{-}MePO_3)^{-2}$ complex, which would require very long computational times. We tried to add a water shell on the $MePO_3$ and not on the Ag_{20} cluster but the water molecules migrated from the nonpolar methyl to the silver cluster during the geometry optimization.

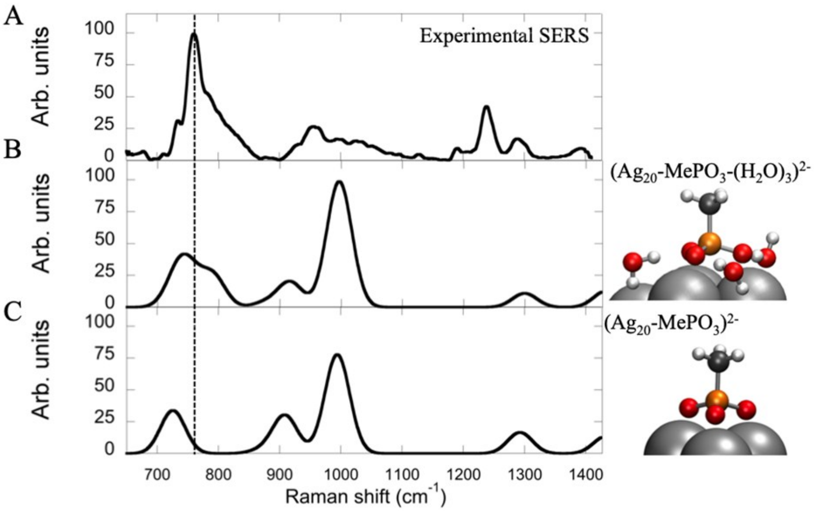

Fig. S2: Experimental SERS spectrum of the methylphosphonate Ag NP complex in solution at pH=9, where the $MePO_3^{2-}$ form dominates. B-C) Raman spectrum of the $(Ag_{20}\text{-}MePO_3)^{2-}$ and $(Ag_{20}\text{-}MePO_3(H_2O)_3)^{2-}$ complexes computed at the DFT/wB97XD level using PCM. The relative intensities are normalized to the highest peak for the experimental spectrum (P-C peak, panel A). For the computed spectra, the relative intensities are normalized to the PO peak (panel B).

Overall, we showed that the discrepancies observed between the Raman spectrum computed with a continuous solvation model (here PCM) and the experimental Raman spectrum of $MePO_3^{2-}$ are due to the explicit interaction of water molecules. We also showed that such interactions are also important for the SERS spectrum. In addition, in SERS, other molecules present in the solution such as the stabilizing agent (H_3BO_3) or hydroxide (depending on the pH) may play a significant role, which should also be accounted for explicitly in the electronic structure computations.

2) Isomers of the analyte-silver cluster complexes

For the molecules investigated here, there are several isomers of the silver-analyte complexes. We differentiate two types of isomers. In the first type, the adsorption of the analyte occurs through different functional groups, which often leads to significantly different Raman spectra and binding energies. The second type of conformers consists in rotation of dihedral angles, which typically leads to small changes of the Raman spectra and binding energies. In the main text we report the lowest energy isomer of the 5 molecules for which a SERS spectrum has been measured, while below we report a selection of isomers for each molecule.

2.1: Complexes $(Ag_{20}\text{-}MePO_3)^{2-}$ and $(Ag_{20}\text{-}MePO_3H)^{-}$

The doubly deprotonated methylphosphonate anion could adsorb on the Ag_{20} cluster either by the phosphonate group or by the methyl side. However, we did not succeed to determine a stable structure where the $MePO_3^{2-}$ is adsorbed on the silver cluster by the methyl. During the geometry optimization, the analyte rotates to eventually adsorb by the doubly deprotonated phosphonate, which is the expected binding site because it forms a stable tripod interaction between the oxygen atoms of the phosphonate and the silver atoms of the cluster. The adsorption by the phosphonate leads to a qualitative agreement with the experimental SERS spectrum, the discrepancies being assigned to the explicit solvation (see section above).

We investigated the effect of the dihedral angle between the phosphonate and the methyl on the Raman spectrum by systematically rotating the methyl from 0 to 120° for the $(Ag_{20}\text{-}MePO_3)^{2-}$ complex. At 0° the methyl and phosphonate are in a staggered conformation while at 60° they are in an eclipsed conformation. The staggered conformation is 2.6 kcal/mol more stable than the eclipse one. Overall the Raman spectra of the two conformers are very close (Figure S3). There is a small effect on the methyl band that is blue shifted by about 25 cm^{-1} for an eclipse conformation compared to the staggered one. The small difference of binding energies and Raman spectra suggest that all these conformers are present in solution.

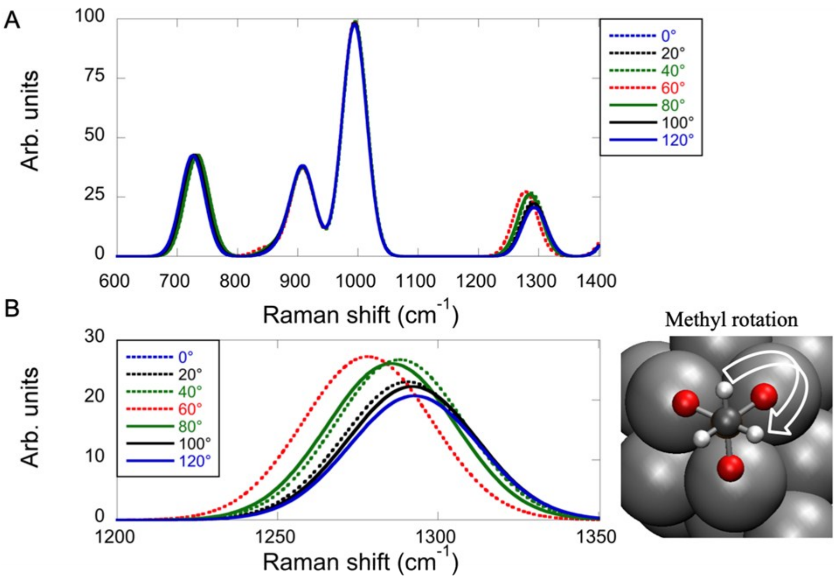

Fig. S3: A) Raman spectrum of the $(Ag_{20}\text{-}MePO_3)^{2-}$ complex computed at the DFT/wB97XD level with PCM for different orientations of the methyl with respect to the phosphonate. The complex labelled 0° corresponds to the lowest energy conformer with a staggered conformation (shown in the panel below). B) Inset of panel A. The relative intensities in panel A are normalized to the highest peak (PO peak).

Like for the $(Ag_{20}\text{-}MePO_3)^{2-}$ complex, the $(Ag_{20}\text{-}MePO_3H)^{-}$ complex adsorbs only by the phosphonate function and the rotation of the methyl only slightly affects the methyl breathing peak around 1300 cm^{-1}.

2.2: Complex $(Ag_{20}\text{-}AMPA)^{2-}$

For the Ag_{20}-AMPA (θ_3) complex, the adsorption of the AMPA anion (with a charge of -2) can occur through the phosphonate (isomer 1) or through both the amine and phosphonate (isomer 2), see Fig. S4. We did not succeed to find stable geometry where the adsorption occurs solely by the amine as the molecule rotates during the geometry optimization to absorb by both the amine and the phosphonate functions (isomer 2). The Raman spectra of the two isomers are shown in Fig. S4B-C and there is a good agreement between the experimental SERS spectrum and the computed spectrum of the isomer 1. The Raman spectrum of the isomer 2 does not have a peak around 750 cm^{-1} that is present in the measured SERS spectrum and it has an additional peak at 1375 cm^{-1} that in not present in the SERS spectrum. Furthermore the adsorption by the phosphonate alone (isomer 1) leads to a complex 5.3 kcal/mol more stable than by both the amine and phosphonate (isomer 2). This seems to indicate that adsorption occurs preferentially as in the isomer 1.

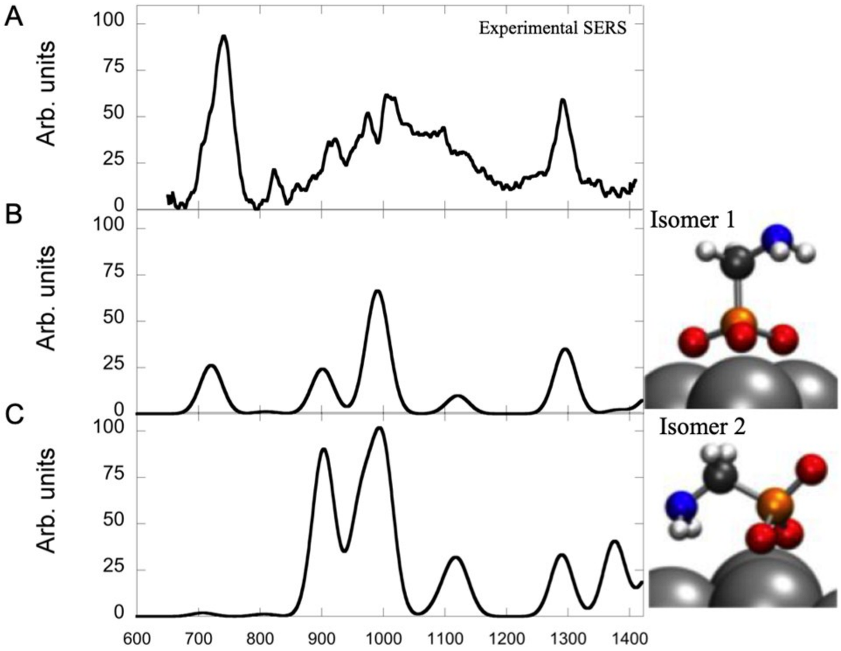

Fig. S4: Experimental SERS spectrum of the AMPA anion in solution at pH=10.5, where there the doubly deprotonated AMPA (θ_3, charge -2) form dominates. B) Computed Raman spectrum of the isomer 1 of the complex ($(Ag_{20}$-$AMPA(\theta_3))^{2-}$ computed at the DFT/wB97XD level with PCM (the equilibrium geometry is shown on the right). C) Same as panel B) for the second isomer. The relative intensities are normalized to the highest peak for the experimental spectrum (P-C peak, panel A). For the computed spectra, the relative intensities are normalized to the PO peak (panel C).

2.3: Complex (Ag_{20}-AMPA)$^-$

For the complex (Ag_{20}-AMPA)$^-$ (θ_2), which is has a negative charge, there are several binding sites (on the phosphonate or on both the phosphonate and the amine) and different protonation sites as the acidic proton can be localized either on the amine or phosphonate (see Fig. S5B-C). The two lowest energy isomers that we identified are adsorbed to the cluster by the phosphonate function. However for the lowest energy isomer (isomer 1, $E_{binding}$ = 21.6 kcal/mol), the proton is localized on the phosphonate (Fig. S5B) and two oxygen atoms mainly interact with two silver atoms of the cluster while for the second isomer (isomer 2, $E_{binding}$ = 15.1 kcal/mol), the amine is protonated (Fig. S5C) and there is a tripod interaction of the three oxygen atoms with three silver atoms of the surface. This leads to a Raman spectrum

(Fig. S1B) with two and one peak between 600 and 900 cm^{-1} respectively. Since there are two peaks in the measured SERS spectrum at pH = 7.5 between 600 and 900 cm^{-1} and that the binding energy of the first isomer is 6.5 kcal/mol more stable than the one of the second isomer, it indicates that the adsorption should occur preferentially as in the first isomer. Nevertheless, given the binding energies and spectra of the second isomer, we cannot rule out that for a fraction of the AMPA molecules adsorbed on the cluster, the proton is localized on the amine.

As for the doubly protonated AMPA form (θ_3), the adsorption of the AMPA θ_2) analyte could occur from both the amine and phosphonate (isomer 3, Fig. 5D) but the Raman spectrum does not correspond qualitatively to the experimental SERS spectrum so this adsorption mode is not likely present in the experiment. The 3rd isomer is less stable (binding energy difference of 3kcal/mol) than the isomer 1.

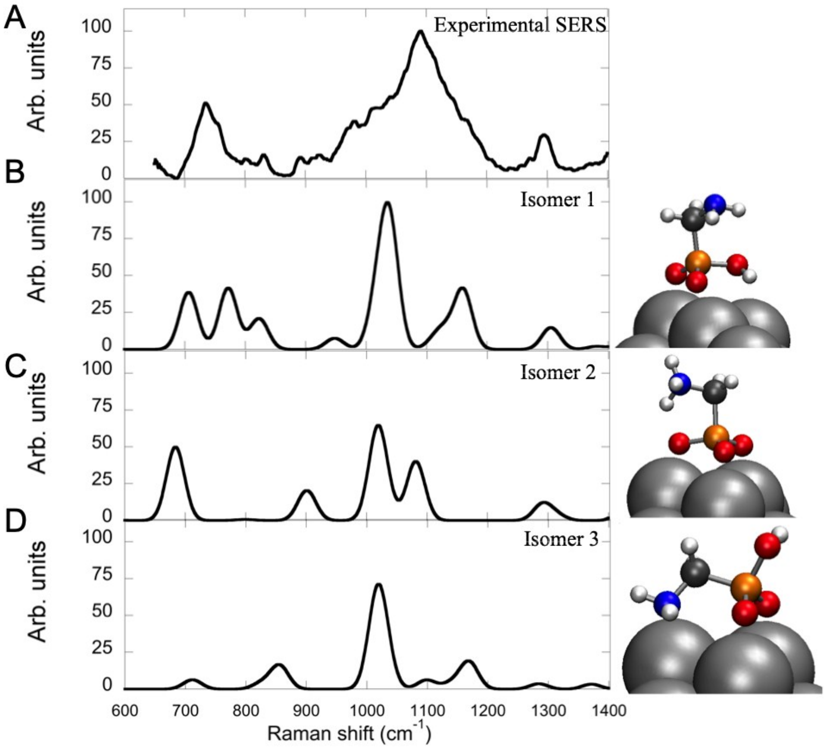

Fig. S5: Experimental SERS spectrum of the AMPA molecule in solution at pH=7.5, where the AMPA$^-$ (θ_2) form dominates. B) Raman spectrum of the isomer 1 of the complex (Ag$_{20}$-AMPA(θ_2))$^-$ computed at the DFT/wB97XD level with PCM (the equilibrium geometry is shown on the right). C) and D) Same as panel B) for the second isomer and third isomer. The relative intensities are normalized to the highest peak, the P-O peak (experimental: panel A, computed: panel B).

We also investigated the effect of rotating the dihedral angle between the phosphonate and the amine moiety on the computed Raman spectrum of the singly deprotonated AMPA (Fig. S6). We started from the lowest energy isomer (isomer 1) and rotated the CH_2-NH_2 moiety by 120° and 240°. There are small changes in the P-C peak (around 750 cm^{-1}) but overall the spectrum is quantitatively the same. The difference of binding energies is relatively small (<2 kcal/mol) indicating that all these conformers are likely present in solution.

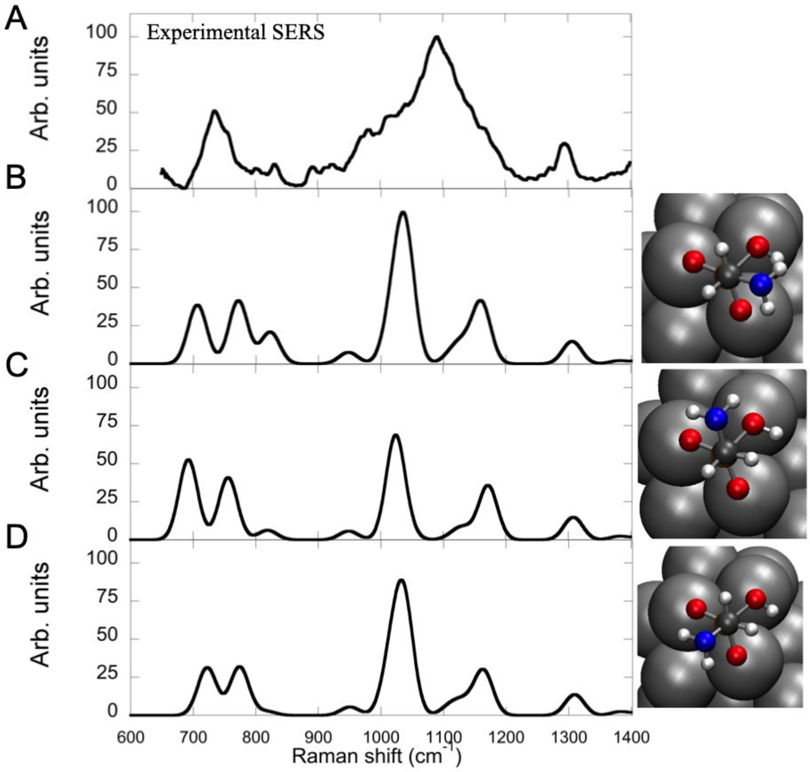

Fig. S6: Experimental SERS spectrum of the $AMPA^-$ (θ_2) molecule in solution at pH=7.5, where there the $AMPA^-$ (θ_2) form dominates. B-D) Raman spectrum of the $(Ag_{20}\text{-}AMPA(\theta_2))^-$ complex computed at the DFT/wB97XD level with PCM for different orientation of the -CH_2-NH_2 moiety with respect to the phosphonate. In panel B, the spectrum is computed for the equilibrium geometry (shown on the right) while in panel C and D the CH_2-NH_2 moiety has been rotated by 120° and 240° respectively. The relative intensities are normalized to the highest peak, the P-O peak, (experimental: panel A, computed : panel B).

2.4: Complex $(Ag_{20}\text{-Glyphosate})^{2-}$

There are several possible isomers of the complex (Ag_{20}-Glyphosate)$^{2-}$ (θ_3). The lowest energy isomer is a complex where the adsorption of the glyphosate occurs through the phosphonate with the glyphosate molecule oriented perpendicularly to the surface (Fig. S7B). The Raman spectrum of this isomer corresponds quite well to the experimental SERS spectrum (Fig. 7A), indicating it should be present in solution. We computed the electronic structure of a second isomer (isomer 2 in Fig. S7C) where the adsorption occurs through the phosphonate and the carboxylate function and where the molecule lies parallel to the surface. The Raman spectrum strongly differs from the one of the lowest energy isomer and from the experimental SERS spectrum. The binding energy of the isomer 2 is only 3 kcal/mol lower (less stable) than the one of the lowest energy isomer (isomer 1) but the Raman spectrum does not correspond well the experimental SERS spectrum, which indicates that this isomer is not likely to be present in solution.

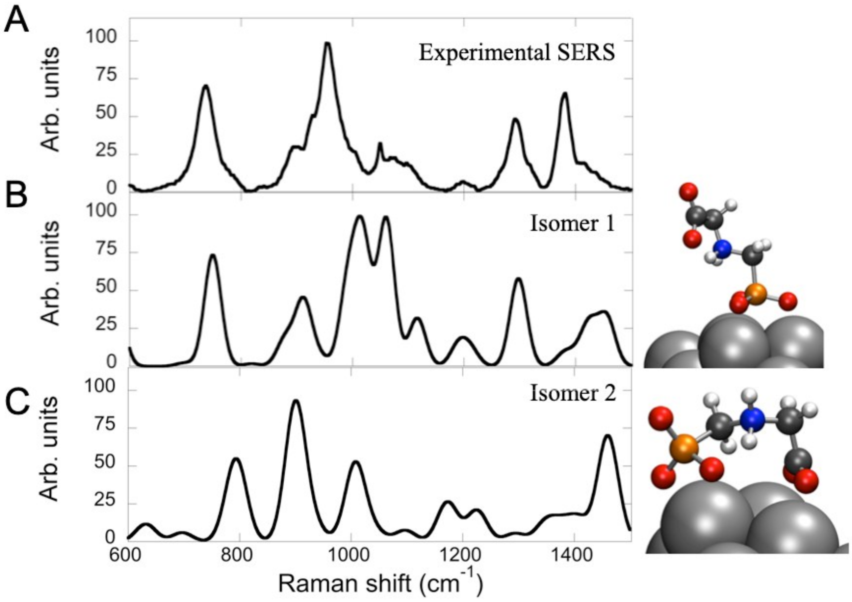

Fig. S7: A) Experimental SERS spectrum of glyphosate at pH = 9 where the θ_3 form dominates. B) Isomer 1 of the (Ag_{20}-Glyphosate)$^{2-}$ complex computed at the DFT/wB97XD level with PCM (equilibrium geometry is shown on the right). C) Same as B but with the isomer 2. The relative intensities are normalized to the highest peak, the P-O peak (experimental: panel A, computed : panel B).

3) Raman spectra between 0 and 2000 cm^{-1}

In the main text, the Raman spectra of the complexes investigated are shown between 600 cm^{-1} and 1400 cm^{-1}. We report here the computed spectra from 0 to 2000 cm^{-1}.

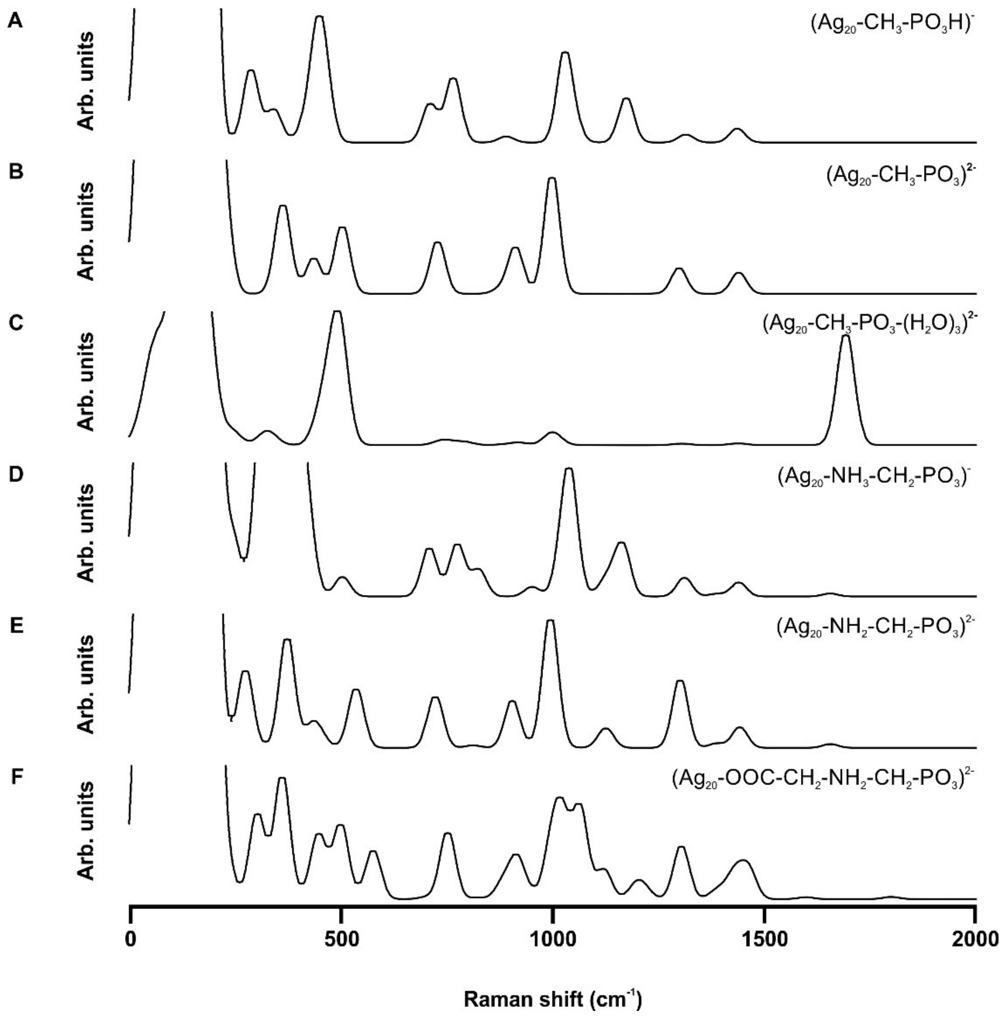

Fig. S8: Computed Raman spectra of complexes between 0 and 2000 cm^{-1} (A) $(Ag_{20}\text{-}CH_3\text{-}PO_3H)^-$, (B) $(Ag_{20}–CH_3–PO_3)^{2-}$, (C) $(Ag_{20}\text{-}CH_3\text{-}PO_3\text{-}(H_2O)_3)^{2-}$, (D) $(Ag_{20}\text{-}NH_3\text{-}CH_2\text{-}PO_3)^-$, (E) $(Ag_{20}\text{-}NH_2\text{-}CH_2\text{-}PO_3)^{2-}$ and (F) $(Ag_{20}\text{-}OOC\text{-}CH_2\text{-}NH_2\text{-}CH_2\text{-}PO_3)^{2-}$